Proceedings of the ASME 2015 International Mechanical Engineering Congress & Exposition
IMECE2015
November 13-19, 2015, Houston, Texas

IMECE2015-51349

RECENT DEVELOPMENTS IN STEEL FRICTION STIR WELDING – PROJECT HILDA

Athanasios I. Toumpis
University of Strathclyde
Glasgow, UK

Alexander M. Galloway
University of Strathclyde
Glasgow, UK

Duncan Camilleri
University of Malta
Msida, Malta

Larbi Arbaoui
Cenaero
Gosselies, Belgium

ABSTRACT

Friction stir welding of steel presents an array of advantages across many industrial sectors compared to conventional fusion welding techniques. Preliminary studies have identified many positive effects on the properties of welded steel components. However, the fundamental knowledge of the process in relation to structural steel remains relatively limited, hence industrial uptake has been essentially non-existent to this date. The European-funded project HILDA, the first of its kind in terms of breadth and depth, is concerned with enhancing the understanding of the process on low alloy steel, establishing its limits in terms of the two more significant parameters which can be directly controlled, tool traverse and rotational speed, thus improving its techno-economic competitiveness to fusion welding.

A detailed study investigated the effect of process parameters on the evolved microstructure. In parallel, a full programme of mechanical testing was undertaken to generate data on hardness, impact toughness and fatigue. From this, it has been established that friction stir welding of steel produces high integrity joints that exhibit excellent fatigue properties.
From a simulation perspective, a local microstructural numerical model has been developed to predict the microstructural evolution within the weld zone during friction stir welding of low alloy steel. This model concentrates on predicting grain size evolution due to dynamic recrystallization with respect to tool traverse and rotational speed. Furthermore, a computational efficient local-global numerical model capable of predicting the thermal transients, stir and heat affected zone, residual stresses and distortion produced by friction stir welding of DH36 plates is presented.

Keywords: Friction stir welding; Low alloy steel; Optimisation; Microstructure, Mechanical testing; Numerical models; Dynamic recrystallization; Residual stresses; Out-of-plane distortion

INTRODUCTION

The principles and merits of friction stir welding (FSW) have been extensively reported [1–3] and the output from this work has seen some growth in the usage of FSW for the light metals. As the process and available tooling has evolved, a significant interest has developed to transfer the process and its advantages from low melting point materials such as aluminium to steel [1]. It has been proposed that the transportation, e.g. in automotive [4] and rail applications, marine, shipbuilding [5], and oil and gas sectors [6] could make use of technical benefits by implementing steel FSW as a high value manufacturing process. Previous publications have demonstrated the feasibility of FSW on steel [1,2], while others report that there are several positive effects on the weld properties such as considerable grain refinement [7], overmatching of the parent metal [2], minimised distortion [8] which translates into reduced re-work of the welded components, and potential for welding speeds which can be technically competitive to fusion welding methods [3]. By avoiding the fusion and subsequent solidification of the metal, FSW can deliver welds free of typical arc welding defects like porosity, solidification cracking and embrittlement [9].

Studies demonstrate that FSW is capable of joining metals that are otherwise considered of low weldability or practically non-weldable by established fusion joining methods. For instance, research [10] notes that welding of high carbon steels demonstrates significant challenges due to their low

weldability, a consequence of the high carbon content. It is concluded that welding of high carbon steels can be successfully accomplished by FSW [10].

The commercial uptake of FSW for structures manufactured from steel is extremely low. One obstacle is the current tool technology, and more specifically the high requirements on the tool material [11]. The material from which FSW tools for high melting point metals are manufactured needs to exhibit sufficient fracture toughness, wear resistance and chemical inertness with respect to the metal to be welded, all at high temperatures [11]. The latest developments in tool technology have yielded hybrid tools consisting of polycrystalline boron nitride (pcBN) particles in a refractory metal (WRe) binder. Still, pcBN tools are presently expensive and demonstrate cracking and wear, thus are known to produce weld lengths that are too short (max. 40 m per tool) to be economically viable for any industry which may be assessing the introduction of the process [12]. Furthermore, the tools for steel presently allow for only two steel joint configurations to be welded, i.e. butt and lap joints. Publications note the current limitations of steel FSW, as outlined above, and conclude that new developments on tool design and materials, and the identification of relevant niche applications which will decisively benefit from the introduction of FSW are the two critical factors for wider industrial use of the process on steel [9].

FSW needs to be optimised with regard to high welding speed of defect-free welds of acceptable quality, within specifications or classification society rules in the case of shipbuilding and marine applications, rather than best possible mechanical properties for wider industrial introduction and a detailed optimisation study is currently available in the public domain [13]. From this study [14] it is proposed that, for FSW of steel to become an economically and technically viable alternative to conventional fusion welding processes, further advances in tooling design (material, geometry and cost) is of fundamental importance.

In parallel with the accepted need for tooling optimisation, a series of process parameter studies with the aim of maximising the rate of welding (based on tool rotation and traverse speed) will be required to support any tooling advances that are realised. For example, few pertinent studies report on the effect of traverse speeds in the range of 200-300 mm/min on the developed microstructure and resultant mechanical properties of structural steels, much less on process optimisation at higher speeds. One indicative publication employs ten parameter sets, with a maximum traverse speed of 200 mm/min, in an optimisation study of the FSW of an advanced high strength steel (AHSS) [4]. Although the tensile shear test samples are seen to fracture in the HAZ, this study does not seek to enhance the tensile properties of this region through the evaluation of refined parameter sets.

In the present investigation and in contrast to previous process parameter development studies, 25 friction stir welds, the majority of which were produced with welding speeds rarely identified by other researchers, are thoroughly examined in order to determine a step change improvement to the current industrially accepted welding speeds. These are selected from a comprehensive and considerable spread of over 200, 2000 mm long FSW DH36 butt joints in which slow, intermediate and fast welding speeds were trialled.

Through this process parameter development, the state of the art has been increased from conventionally adopted welding speed of 100 mm/min to more commercially attractive speeds in the region of 400 mm/min – 500 mm/min. However, welding is known to substantially affect the microstructure and mechanical properties of components and structures [14]. Although a step change in the welding speed has been identified, the purpose of the research work presented herein is to assess the impact of this increase on the microstructural evolution and mechanical properties of each friction stir weld. Furthermore, with the aid of local and global modelling techniques that have been fully validated within the present study, the model outputs are capable of predicting the sensitivity of process parameter adjustments as a function of microstructure evolution, distortion and residual stresses.

EXPERIMENTAL PROCEDURES

Material and welding details

More than 200 single sided friction stir welds in 6 mm thick DH36 steel were produced using a PowerStir FSW machine operated in position control. Steel plates with original dimensions of 2000 mm x 200 mm were securely clamped on the machine bed in a square edge butt joint configuration without any prior surface preparation and butt welded together at varying traverse speeds using hybrid WRe-pcBN stepped spiral tools to form a steel component of 2000 mm x 400 mm. The welding parameters used in this study are grouped in three categories which will subsequently be referred to as “slow”, “intermediate” and “fast”.

Microstructure evaluation

Microstructural characterisation was undertaken to generate important information regarding the mechanical properties that are likely to be attained in the weld zone and to identify any undesirable process induced flaws or defects that could compromise the integrity of the weld. One metallographic sample was transversely sectioned from a random position within the steady state condition region of each examined weld and prepared using normal met-prep equipment and consumables, and in a way that the advancing (AD) side is seen on the left side of all images. Macrographic images of the weld were captured and a detailed examination of areas of interest within the weld region identified on the macrographs was performed using an optical microscope.

Tensile testing

Three transverse tensile tests per weld were conducted on an Instron 8802 uniaxial tensile testing system in accordance with ISO Standards [15] to determine the yield strength (YS) and UTS that the applied sets of weld parameters produce on the welded plates, along with the position of fracture (parent

material or weld metal).

Hardness and impact toughness

Micro-hardness measurements were recorded for each welding speed and in several positions which were deemed representative of the weld zone (Fig. 1) to provide an understanding of the hardness distribution of the weld zones, hence information relevant to the behaviour during mechanical testing. The measurements were taken using a Mitutoyo hardness tester and by applying a load of 200 gf.

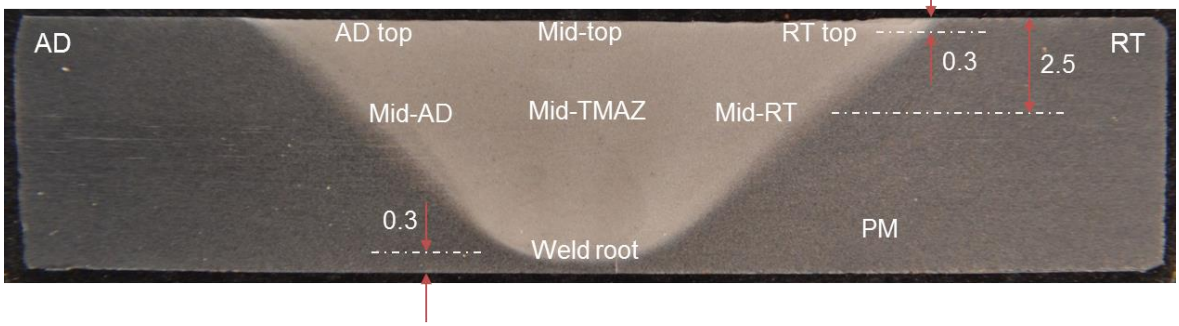

Fig. 1. Typical FSW macrograph with the positions of hardness measurements

Charpy impact tests with the standard V-notch were performed according to ISO Standards [16] in order to evaluate the toughness of the weld region in relation to the applied parameter sets. Samples were sectioned perpendicular to the weld centreline and transverse to the weld direction. One sample was sectioned with the notch axis of symmetry on the weld centreline. To examine the full width of the weld region, three additional samples were sectioned towards both sides of the weld and with the position of the notch axis of symmetry in 1.5 mm increments. Reduced-section samples of 5 mm width were used due to the plate thickness of 6 mm [16]. In total, three sets of seven tests were performed for each set of parameters to improve the accuracy of the results.

Fatigue testing

There are no internationally accepted standards for the testing and assessment of welded components under fatigue [5], apart from guidelines. The lack of such standards is even more evident with regards to investigating the FSW of steel [17], a novel process. Thus, a comprehensive set of guidelines for the fatigue assessment of FSW of steel were developed. This allowed for a fully compliant fatigue testing programme to be performed. Three welds of parameters which were deemed representative of each welding speed group (Tab. 1) were produced specifically for the fatigue testing programme. The selection of appropriate stress ranges was informed by trial tests which were initially performed, commencing with stress range of 80% of YS. The effect of varying FSW parameters on the fatigue lives was established by testing samples from the slow and fast speed welds at one stress range and comparing these results with the basic *S-N* data of the intermediate weld. The stress ratio was maintained approx. equal to 0.1 and the stress frequency constant at 10 Hz during the testing programme. The actual stresses attained by the testing machine vary insignificantly from the calculated values (no more than 0.1%).

Tab. 1. Number of tested fatigue samples per welding speed

Weld reference	Traverse speed (mm/min)	Rotational speed (rpm)	Stress range (% of YS)	Number of tested samples
Intermediate	250	300	90	10
			80	10
			70	5
Slow	100	200	80	3
Fast	500	700	80	3

RESULTS AND DISCUSSION

Microstructural characterisation

The characteristic equiaxed ferrite/pearlite banded microstructure of DH36 steel is displayed in Fig. 2a. The slow welds (in the range of 100-200 mm/min) present a defect-free and homogeneous ferrite rich microstructure with highly refined grains of random geometry.

A small content of apparently acicular shaped bainitic ferrite is developed by the 120 mm/min welding speed (Fig. 2b), and this is seen to steadily increase with increasing traverse speed. This observation confirms that the cooling rate

is increasing with increasing traverse speed. Such acicular shaped bainitic ferrite thermo-mechanically affected zone (TMAZ) microstructure has been reported previously [6] for similar welding speeds, developed as acicular bainitic ferrites nucleate mainly on the austenite grain boundaries. It is noted that this is a product of the phase transformation of austenite, in the supercritical stir zone (central TMAZ), to ferrite at a high cooling rate [6].

The microstructure becomes more heterogeneous in the intermediate group of welds (250-400 mm/min), with regions of increasing bainite content (suggesting increased cooling rates). Nevertheless, the weld at 350 mm/min features a homogeneous, fully acicular bainitic ferrite microstructure (Fig. 2c); this suggests that a good balance of rotational and traverse speed has been achieved. In addition, prior austenite grain boundaries can be observed on the light optical microscope (Fig. 2c).

At the high welding speeds of 450 & 500 mm/min, the microstructure of all examined welds is heterogeneous, with poorly mixed regions of acicular ferrite and varying bainite content (Fig. 2d). The presence of bainite has increased considerably in this group due to the even higher cooling rate that is occurring. Prior austenite grain boundaries are detected on the regions of bainite predominant microstructure (Fig. 2d).

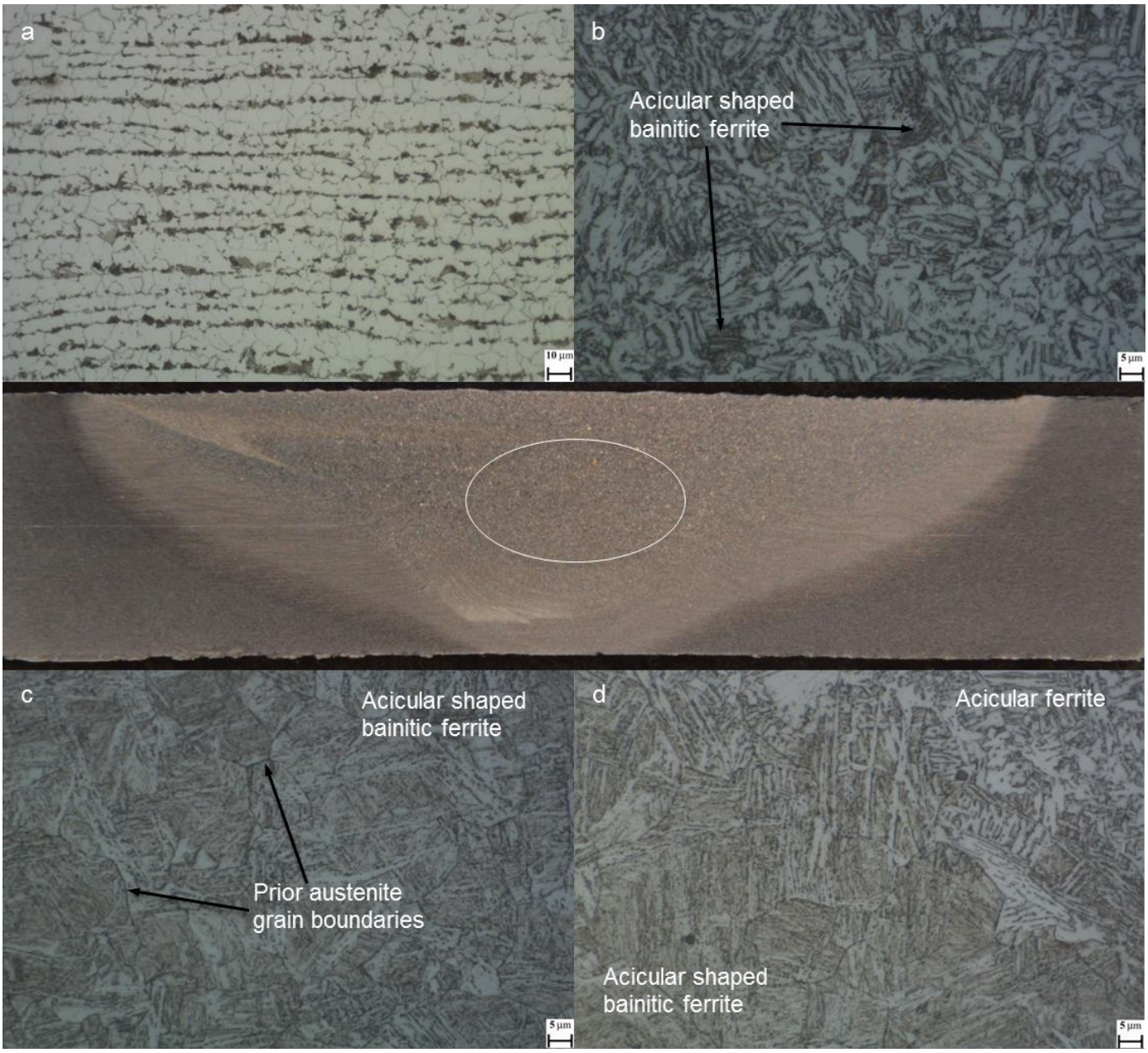

Fig. 2. Microstructure of (a) parent material [x500, Etched]; mid-TMAZ (b) 120 mm/min [x1000, Etched]; (c) 350 mm/min [x1000, Etched]; (d) 500 mm/min [x1000, Etched]

A separate study concludes that this acicular shaped microstructure is a consequence of the phase transformation of austenite during fast cooling from a peak temperature above the upper transformation temperature (A_3) [2].

A number of the intermediate and fast speed welds exhibit incomplete fusion paths on the AD side, within which interconnected non-metallic inclusions are detected (Fig. 3a). These flaws are expected to impact on the mechanical properties of the welds, particularly their fatigue performance. Moreover, some samples disclose minor weld root flaws (Fig. 3b), i.e. regions of insufficient or no welding of the original interface between the two plates. These types of flaws are regarded as processing features and are expected to be resolved as the technical expertise on FSW of steel gradually develops. Still, no embedded flaws are detected in the bulk of the weld zone (TMAZ), thus high speed friction stir welding of steel grade DH36 is feasible at a wide range of traverse speeds.

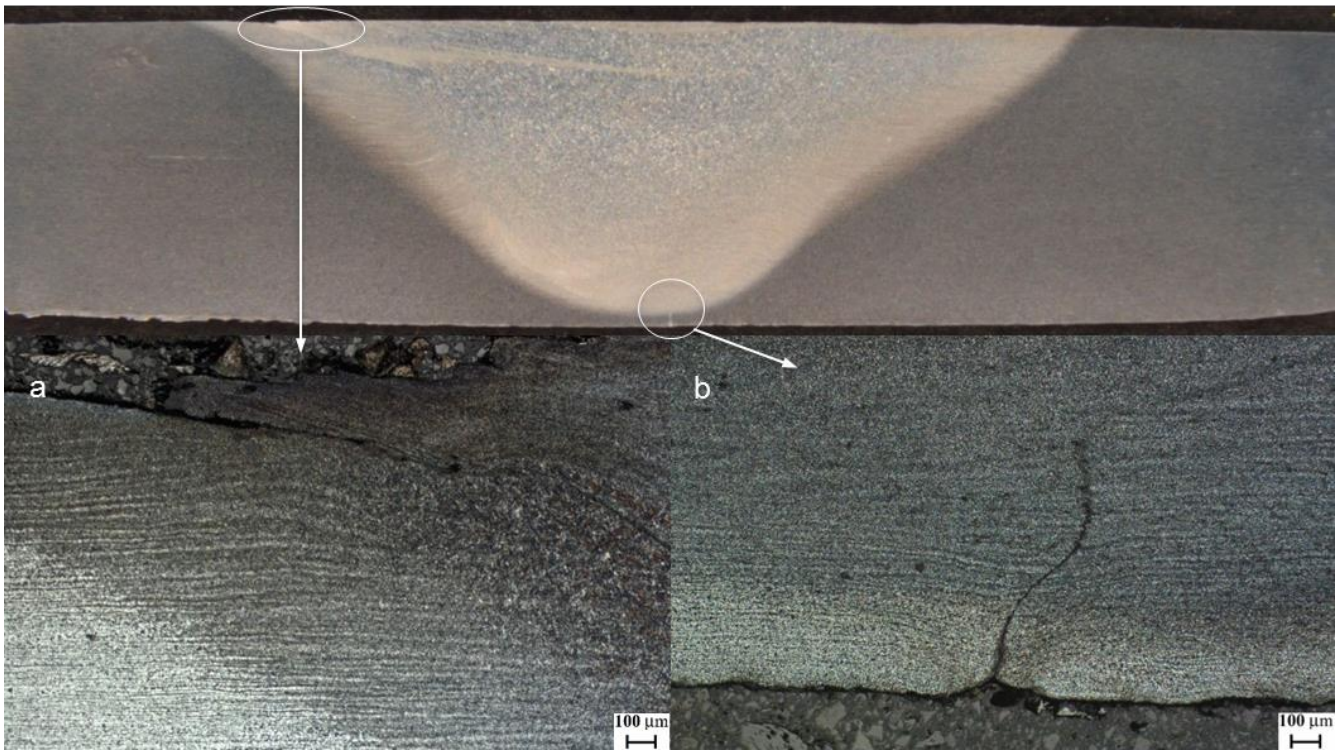

Fig. 3. Weld flaws [x50, Etched], (a) incomplete fusion; (b) weld root flaw

Tensile properties

The samples of 19 out of the 25 welds, including all samples prepared from the 18 slow and intermediate welds, fractured in the parent material rather than the weld similar to previous studies [2,7,8]. This demonstrates that these 19 sets of weld parameters produced welds of higher strength than the parent material. Even welds with minor process related flaws, or welds which consist of high acicular bainitic ferrite phase ratio and therefore could be expected to show brittle behaviour proved to be stronger than the parent material. An average yield strength value of 382 MPa was calculated from the slow and intermediate groups, and used in the fatigue testing parameters to offer consistency and comparable results.

The group of fast welds (450 & 500 mm/min) demonstrated a different behaviour, with all samples from 4 parameter sets fracturing in the weld, and specifically in a brittle-like manner on the outer boundary of the AD side. This fracture site corresponds to regions where non-metallic inclusions were found to be interconnected in an incomplete fusion characteristic. Two more parameter sets' samples fractured either inside the weld or the parent material; such tensile behaviour indicates that these sets of parameters are on a threshold value producing welds where steady state conditions have not been reached. Still, all 3 samples from one of the fast welds fractured in the parent material with a typically ductile fracture. It seems that this set of parameters delivered a suitable ratio of traverse and rotational speed that is translated into satisfactory tensile behaviour.

Hardness distribution

Tab. 2 summarises the micro-hardness measurements for three welds as representative of the three traverse speed groups examined; the values are supplied as an average of two measurements per position (Fig. 1). Overall, the hardness values are in agreement with the microstructural observations; the hardness of the weld is seen to increase as the welding speed is increased. This is attributed to the increasing cooling rate which develops harder phases such as bainite. The microstructural examination above has noted the rise in the

bainite content with each speed increment.

Impact toughness measurements

The impact toughness data for 6 indicative welds presented in Tab. 3 have been normalised to a 10 x 10 mm equivalent by a scaling factor of 3/2, as discussed by McPherson *et al.* [8]; the values are provided as an average of three measurements each. The impact toughness of most welds at 20°C is seen to be reduced compared to the parent metal (Tab. 3). The slow welds (100-200 mm/min) follow a similar pattern of peak values on the weld centreline and lowest values nearing both sides of the TMAZ. The intermediate (350-375 mm/min) and fast (500 mm/min) welds exhibit a similar trend in impact toughness distribution, with a peak in the inner TMAZ of the AD side and gradual decrease towards the outer boundaries of the TMAZ on both sides. The homogeneous acicular bainitic ferrite microstructure observed in the 375 mm/min weld has produced marginally higher impact toughness in the AD TMAZ than the heterogeneous microstructure of 500 mm/min. Two sets of parameters overmatch the parent plate's impact toughness in the inner AD TMAZ.

The data in Tab. 3 reveal that increasing the traverse speed from 100 mm/min to 375 mm/min and 500 mm/min is seen to improve the impact toughness on the AD side, although having a lesser effect on the retreating (RT) side. The impact toughness on both sides of the outer TMAZ however is seen to decrease to some extent with the intermediate and fast traverse speed. Still, the improvement in impact toughness offers a level of confidence in increasing the FSW traverse speed.

Tab. 2. Indicative micro-hardness (Vickers, 200 gf) measurements for three welds

Weld	AD top	Mid-top	RT top	Mid-AD	Mid-TMAZ	Mid-RT	Weld root	Parent material
Slow	225	247	244	230	226	222	225	189
Intermediate	302	257	247	266	265	247	240	169
Fast	320	303	318	306	355	356	250	184

Tab. 3. Impact toughness distribution in the weld region for 6 indicative welds, in J

Weld parameters		**Advancing side**			**Centreline**	**Retreating side**		
Traverse speed (mm/min)	Rotational speed (rpm)	**4.5**	**3**	**1.5**	**0**	**-1.5**	**-3**	**-4.5**
100	200	90.8	83.0	74.5	112.0	78.3	79.5	105.3
200	400	107.5	39.8	37.3	101.0	51.0	48.0	43.5
350	450	67.3	79.5	102.0	92.0	92.8	73.5	69.0
375	400	65.5	76.3	134.0	91.0	81.0	76.5	65.3
500	700	80.5	84.5	127.0	106.0	94.5	66.8	66.0
500	675	75.0	82.5	119.0	96.0	92.0	64.0	66.5
Parent material		122.5						

Fatigue assessment

The *S-N* data of the 3 welds' samples are plotted as fatigue life (in number of cycles to fracture) vs. nominal stress range value for each sample in double logarithmic scale (Fig. 4). In order to understand the relevance of the above reported results, these need to be placed in the context of international regulations and specifications. In the maritime sector for instance where the fatigue performance of welded joints is of critical importance, most pertinent class society rules are based on the recommendations of the International Institute of Welding (IIW) for fusion welds [18]. A series of design related fatigue classes (FAT classes) have been established to ensure safe operation of the welded joints during their effective service life. The FAT classes define the cyclic stress range that will not result in fracture within $2 \cdot 10^6$ cycles at a 97.7% probability for various structural details. The fatigue loading mechanism and related design aspects of friction stir butt welds are essentially equivalent to conventional fusion welds. Thus, FSW needs to be initially evaluated and compared to the established class rules for fusion welding for the process to be considered for marine applications.

The solid line in Fig. 4 indicates the IIW FAT 80 weld detail class for single sided butt welded joints at 97.7% probability of survival. The fatigue strength of the FAT 80

class at $2 \cdot 10^6$ cycles is 80 MPa; the slope is m=3 according to the IIW recommendations. The dotted lines represent the probability of survival at 97.7%, 50.0% (mean) and 2.3%. The results demonstrate higher fatigue strength for all samples of the three welding speeds in comparison to the FAT 80 class. The FSW samples' fatigue strength is calculated at 125 MPa (for 97.7% probability of survival); this is 56% higher than the strength stated in the IIW recommendations. This testing programme reveals an excellent picture of FSW of low alloy steel, with all tests reaching well above 10^5 cycles, the original objective of this investigation.

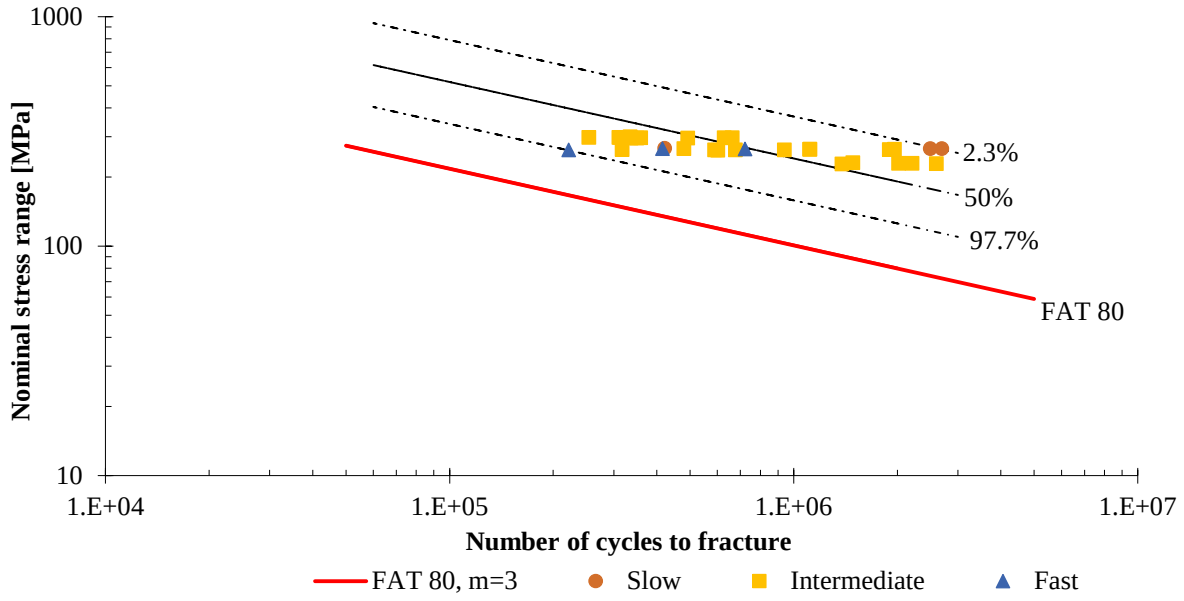

Fig. 4. *S-N* curve of the three welds compared to the IIW FAT 80 class

LOCAL MICROSTRUCTURAL MODEL

The experimental observations such as the microstructural characterisation study have informed the development of the local model. Relevant microstructural evaluation has highlighted the impact of metallurgical phenomena such as DRX on the final weld. In order to model the resulting grain refinement, a phenomenological model has been used and adapted for the FSW of low alloy steel.

A two-step model

The thermo-mechanical local phenomena which occur during the welding stage of the process are described by a thermo-fluid model. This local model based on flow formulation is implemented to simulate the velocity and temperature distribution induced by the stirring action of the rotating tool between the materials being welded. The temperature distribution and material flow are computed by solving the continuity, momentum and energy equations for incompressible flow with appropriate boundary conditions and contact/friction condition. This contact/friction condition consists of modelling the friction between the rotating FSW tool and steel workpieces which produces friction shear stresses and frictional heat. This local model can measure the impact of process parameters on the temperature distribution during FSW as shown in Fig. 5. The thermo-fluid model provides the metallurgical model with the velocity and temperature distribution in order to predict grain size evolution induced by DRX. The prediction of the grain size evolution is addressed by a JMAK model which takes into account the discontinuous DRX.

Microstructural model & grain size

The microstructural model is composed of a "streamlines" generation model and a grain size evolution model. This model allows for predicting the microstructural evolution due to strain and thermal cycles. The streamlines algorithm is performed after the thermo-fluid model in order to determine temperature, strain rate and strain cycles. These cycles are extracted along particle path lines during FSW using the streamlines algorithm. The grain evolution is modelled by the JMAK relation which describes the stages of discontinuous DRX, i.e. nucleation, growth and impingement. The onset criterion based on critical strain and the progression of the recrystallized fraction based on nucleation and growth rate depend on temperature, strain, strain rate and initial grain size. The recrystallized grain growth is only a function of the thermo-mechanical conditions and is independent of the initial microstructure.

Sensitivity analysis based on experimental process envelope

A numerical sensitivity analysis has been undertaken to evaluate the influence of process parameters such as traverse and rotational speed on FSW. These two significant process parameters control the heat generation, yielding and cooling rate within the weld zone. A wide range of process parameters has been explored as a result of the thermo-fluid and the

microstructure evolution models. Three groups of parameter sets which originate from the envelope determination of acceptable weld quality have been studied: slow, intermediate and fast groups. The results of the sensitivity analysis in terms of maximum temperature map, recrystallized fraction and grain size are illustrated in Fig. 6, in which each group is represented by one set of process parameters. The maximum temperature map is generated by taking the maximum value from temperature cycles attached to the particle of the welded joint. The HAZ can be determined from this maximum temperature map. The extent of HAZ is far more pronounced in the slow parameters and reduced with the increase in traverse speed. The observations on temperature distributions have shown that the heating and cooling rates are driven by the rotating and traverse velocity respectively.

The dynamically recrystallized zone is attenuated by accelerating the process. For the slow group, the grain refinement covers the entire TMAZ. By increasing the rotational and traverse speed, DRX is restricted in the top surface and the AD side. This analysis concludes that the slow welds present the most homogeneous and refined microstructure. Increasing the traverse speed tends to degrade this homogeneity towards a more heterogeneous and asymmetric microstructure between the AD and RT side; these results are in good agreement with the microstructural characterisation discussed previously.

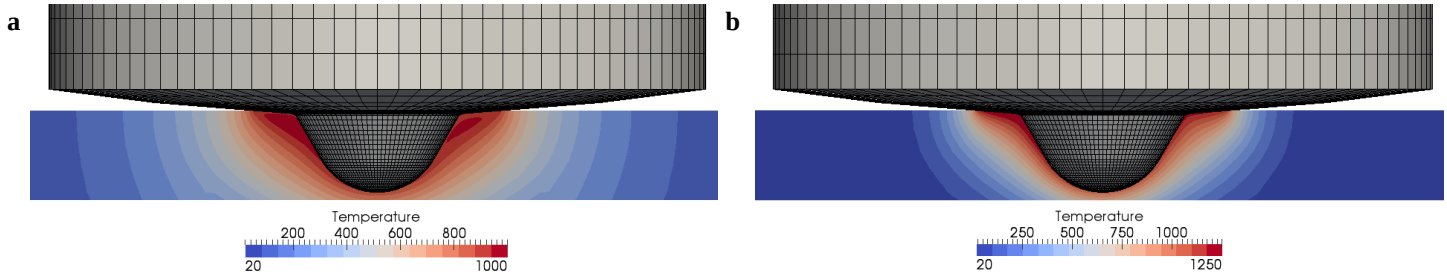

Fig. 5. Temperature distribution during FSW in the vicinity of the tool for (a) 100 mm/min – 200 rpm; (b) 400 mm/min – 500 rpm

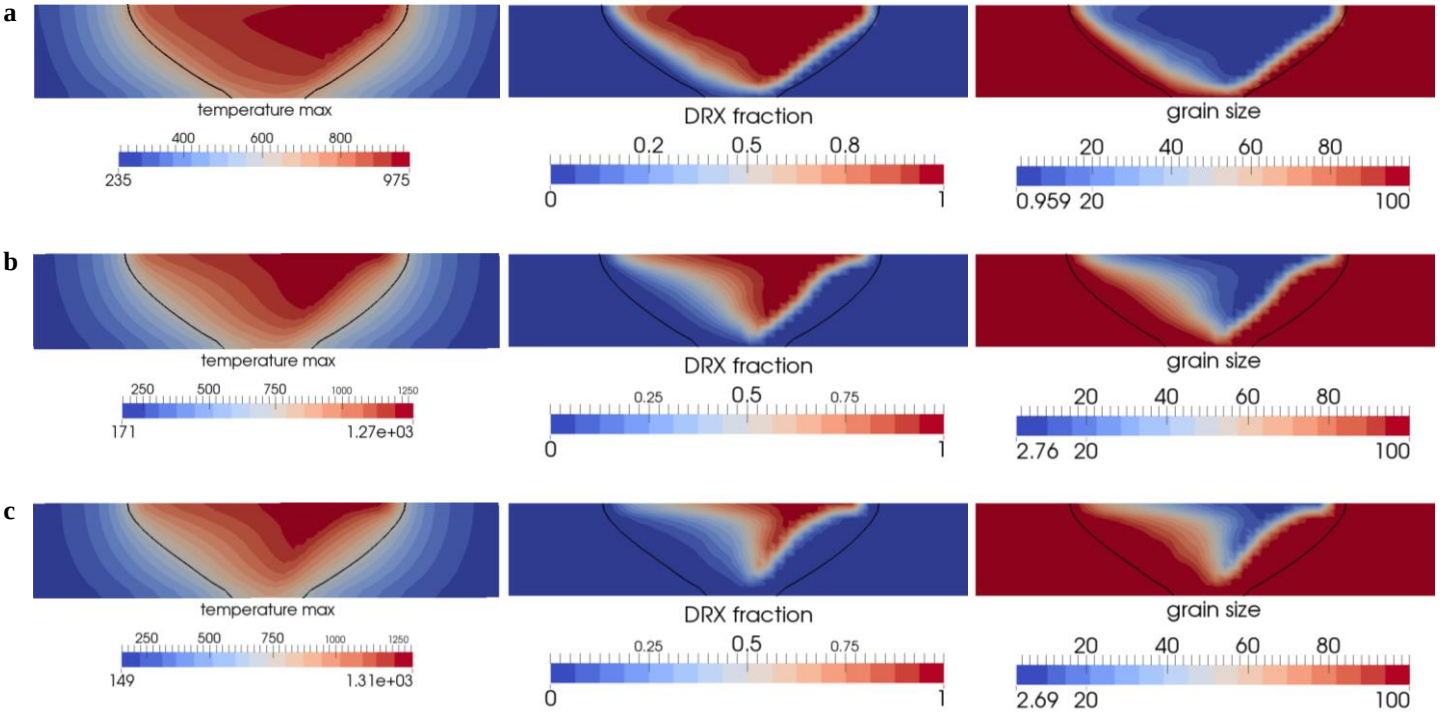

Fig. 6. Temperature map, dynamically recrystallized fraction and grain size distribution for (a) slow (100 mm/min – 200 rpm); (b) intermediate (350 mm/min – 450 rpm); (c) fast (500 mm/min – 575 rpm) welds

LOCAL-GLOBAL NUMERICAL MODELS FOR THE PREDICTION OF RESIDUAL STRESSES AND DISTORTION

Numerical modelling provides an efficient and cost effective tool that is able to predict the temperature evolution, inherent residual stresses and distortion developed due to FSW [19]. A coupled multi-physics numerical model capable of

simulating the interaction between generated heat, material flow, metallurgical evolution, visco-plastic and elasto-plastic structural response is required to fully capture the different physical phenomena present in FSW [20]. However some interactions are weak and can be significantly simplified. For example the thermal properties of the parent material are relatively independent of strain rate and material flow. Furthermore, adopting a fully coupled approach requires significant computational power and time, defeating the purpose of a numerical model capable of predicting residual stresses and distortion [19].

analytical solutions is highly dependent on the accurate definition of empirical variables such as shear stress or kinematic co-efficient of friction [21]. This can be achieved through comparison and reverse engineering, with experimental thermocouple results. On the other hand, the stir/HAZ shape can be defined through macrographic images of welds [3]. However, it is not always possible to have such test results and a means to fully predict the generated heat and stir/HAZ shape is required. This can be achieved through a local visco-plastic computational fluid dynamics model where the shear, material flow, generated heat and stir/HAZ shape for

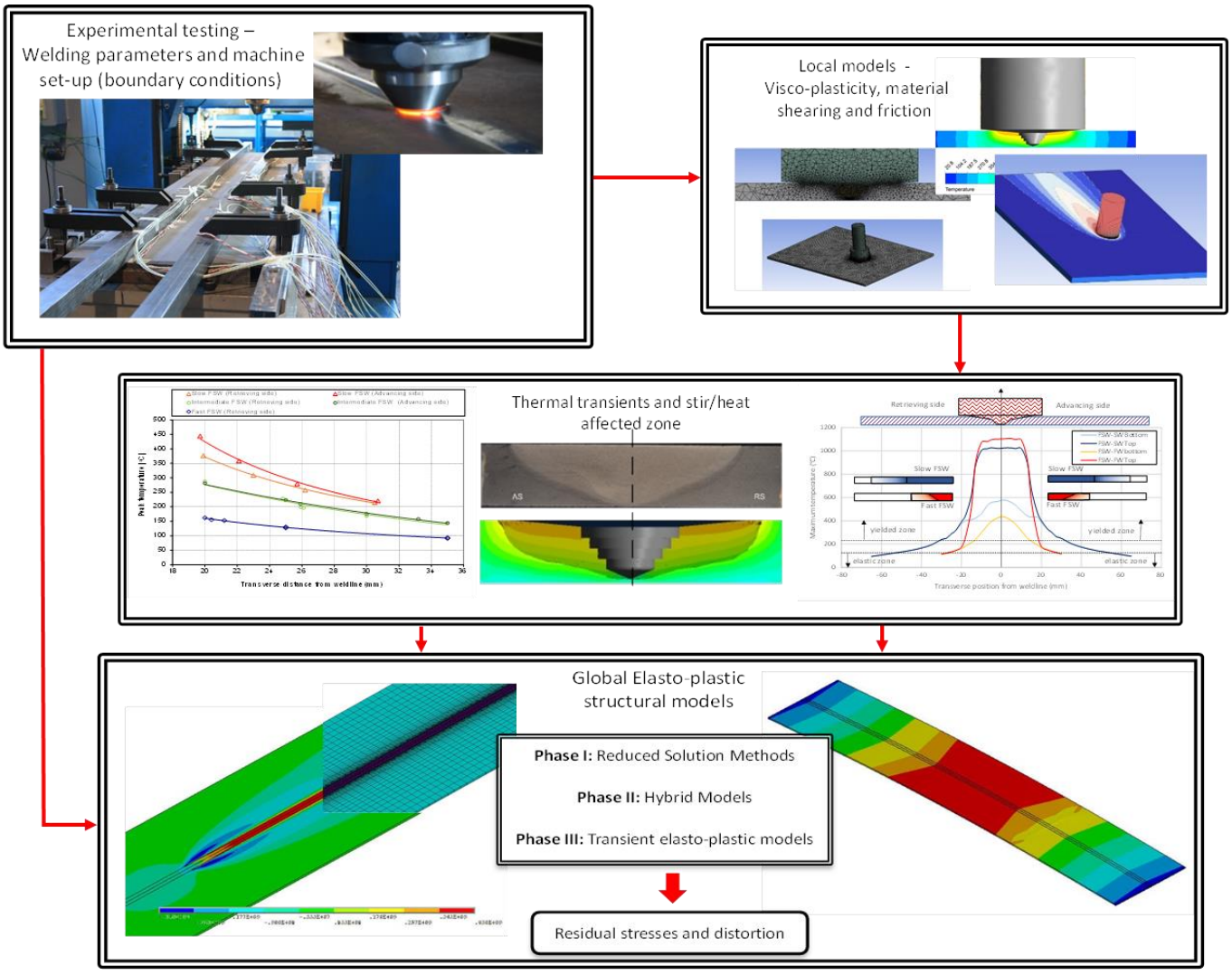

Fig. 7. Numerical modelling strategy and integration between local and global models

A sequentially uncoupled local CFD-global thermo-elasto-plastic FEA model shown in Fig. 7 is therefore adopted and applied to FSW of DH36 steel. In the first instance, the heat generated during FSW and the stir/HAZ shape have to be identified. This can be performed in various ways; for instance, analytical solutions that define the generated heat during FSW are available. Nonetheless, the accuracy of such

specific welding parameters are first predicted [22]; this model is described in this section. Through this modelling strategy's influences due to heat sink parameters, tool shape and welding parameters can be investigated in terms of thermal transients developed during welding.

The predicted thermal gradients are then fed into a global structural model for final prediction of residual stresses and

distortion. Here, the full plate stiffness properties including clamping boundary conditions are simulated. Three numerical modelling strategies ranging from computationally efficient analytical models to more complex transient elasto-plastic numerical models have been developed and investigated. These include:

- Phase I models: Reduced solution methods based on elasto-plastic analytical algorithms [23] that identify FSW contraction forces and applied to elastic static room temperature material properties structural models.
- Phase II models: Hybrid models [24] that take into account non-linear material properties but solved in a two-step heating and cooling cycle in a static manner.
- Phase III models: Transient elasto-plastic models that apply the developed thermal strains in a transient manner with non-linear material properties included.

To maintain confidence in the adopted numerical approach, the numerical models are cross-referenced to realistic test results. In the first instance, the thermal transients developed during welding were measured by means of thermocouple arrays. These measurements provided an insight on the amount of heat being generated, together with highlighting the significant influence of heat loss to the machine bed which is acting as a massive heat sink and ultimately affecting the final residual stress and distortion outcomes. In fact, temperatures in excess of 500˚C where recorded on the machine bed. Effects due to phase transformations and plastic strains are incorporated in the structural models by applying the appropriate material properties that are dependent on the cooling rates developed after welding. The predicted thermal strains, residual stresses and distortion are also validated through a series of strain gauge measurements, hole-drilling residual stress measurements and distortion surface topology measurements.

Reduced solutions provide a cost efficient method of identifying the out-of-plane distortion through simple analytical solutions following elasto-plastic algorithms. These models are capable of identifying the welding contraction forces developed due to FSW and, when applied to an elastic structural model, are able to predict the out-of-plane distortion. Due to the application of fictitious thermal loading and the use of room temperature material properties, their accuracy is limited. Still, these models are capable of giving an insight on which process parameter will lead to less distortion. On the other hand, transient models can fully model the evolution of strains and stresses where influences due to clamping, volume changes due to phase transformation and elasto-plastic temperature dependant material response are taken into consideration. The results attained through these models are in good agreement with the experimental test results but are highly computationally intensive. To this end, hybrid models were developed that take into account all material non-linearities but are solved in a three step heating, cooling and unclamping phase. The results from the hybrid models are also in good agreement with the experimental test results and provide the option to numerically analyse friction stir welded joints that are possibly in excess of 6 m long. These models allow designers and industrial users to assess FSW in a fast and accurate manner.

The combination of experimental and numerical analysis provides a thorough understanding and advancement in knowledge on friction stir welding. For example, both experimental and numerical models have shown that faster traverse speeds in friction stir welding do not necessary lead to less out-of-plane distortion. Other influencing parameters such as heat sink and clamping boundary conditions, workpiece stiffness and support configurations affect the final residual stress and distortion outcomes that can be investigated using a local-global numerical approach.

CONCLUSIONS

The following outcomes are drawn from this extensive research programme:

- FSW of DH36 steel produces an array of highly attractive metallurgical and mechanical properties.
- The industrially accepted welding speed of 100 mm/min for steel has been increased by a factor of 2-3. This step change represents considerable potential economic advantages in terms of the competitiveness of FSW.
- FSW generates a very complex metallurgical system in which the slow traverse speeds result in a very refined, ferrite rich microstructure, the intermediate traverse speeds produce predominantly acicular bainitic ferrites, and the fast traverse speeds result in a heterogeneous microstructure with distinct regions of acicular ferrite and acicular bainitic ferrite.
- Extensive fatigue testing has established that friction stir welds of steel grade DH36 exhibit satisfactory fatigue lives, even at a stress range of 90% of yield strength, above the weld detail class of the International Institute of Welding for fusion welded butt joints.
- A fully validated local microstructural model has been developed and the qualitative influence of process parameters has been investigated through a sensitivity analysis of the microstructural model.
- Local – global numerical models have shown that faster traverse speeds in friction stir welding do not necessarily lead to less out-of-plane distortion, but factors such as heat sink, clamping boundary conditions, workpiece stiffness and support configurations affect the final residual stress and distortion outcomes.

ACKNOWLEDGEMENTS

The authors gratefully acknowledge the financial support of the European Union which has funded this work as part of the Collaborative Research Project HILDA (High Integrity Low Distortion Assembly) through the Seventh Framework Programme (SCP2-GA-2012-314534-HILDA).

REFERENCES

[1] Thomas, W. M., Threadgill, P. L., and Nicholas, E. D., 1999, "Feasibility of friction stir welding steel", Sci. Technol. Weld. Join., 4, pp. 365-372.

[2] Reynolds, A. P., Tang, W., Posada, M., and Deloach, J., 2003, "Friction stir welding of DH36 steel", Sci. Technol. Weld. Join., 8, pp. 455-460.

[3] Toumpis, A., Galloway, A., Cater, S., and McPherson. N., 2014, "Development of a process envelope for friction stir welding of DH36 steel - A step change", Mater. Des., 62, pp. 64-75.

[4] Ghosh, M., Kumar, K., and Mishra, R. S., 2012, "Process Optimization for Friction-Stir-Welded Martensitic Steel", Metall. Mater. Trans. A, 43, pp. 1966-1975.

[5] Azevedo, J., Infante, V., Quintino, L., and dos Santos, J., 2014, "Fatigue Behaviour of Friction Stir Welded Steel Joints," Adv. Mater. Res., 891-892, pp. 1488-1493.

[6] Cho, H-H., Kang, S. H., Kim, S-H., Oh, K. H., Kim, H. J., Chang, W-S., et al., 2012, "Microstructural evolution in friction stir welding of high-strength linepipe steel", Mater. Des., 34, pp. 258-267.

[7] Lienert, T., Stellwag, W., Grimmett, B., and Warke, R., 2003, "Friction stir welding studies on mild steel", Weld. J. Res. Suppl., 1–9.

[8] McPherson, N., Galloway, A., Cater, S., and Hambling, S., 2013, "Friction stir welding of thin DH36 steel plate, Sci. Technol. Weld. Join., 18, pp.441-450.

[9] Barnes, S. J., Bhatti, A. R., Steuwer, A., Johnson, R., Altenkirch, J., and Withers, P.J., 2012, "Friction Stir Welding in HSLA-65 Steel: Part I. Influence of Weld Speed and Tool Material on Microstructural Development", Metall. Mater. Trans. A, 43, pp. 2342-2355.

[10] Chung, Y. D., Fujii, H., Ueji, R., and Tsuji, N., 2010, "Friction stir welding of high carbon steel with excellent toughness and ductility", Scr. Mater., 63, pp. 223-226.

[11] Wang, J., Su, J., Mishra, R. S., Xu, R., and Baumann, J. A., 2014, "Tool wear mechanisms in friction stir welding of Ti–6Al–4V alloy", Wear, 321, pp. 25-32.

[12] Toumpis, A., Galloway, A., Cater, S., and Molter L., 2014, "A techno-economic evaluation of friction stir welding of DH36 steel", Proc. 10th Int. Frict. Stir Weld. Symp., Beijing, China.

[13] Fraser, K., St-Georges, L., and Kiss, L., 2014, "Optimization of Friction Stir Welding Tool Advance Speed via Monte-Carlo Simulation of the Friction Stir Welding Process", Materials, 7, pp. 3435-3452.

[14] Schaumann, P., and Collmann, M., 2013, "Influence of Weld Defects on the Fatigue Resistance of Thick Steel Plates", Procedia Eng., 66, pp. 62–72.

[15] British Standards Institution, 2009, "BS EN ISO 6892-1. Metallic materials – Tensile testing – Part 1: Method of test at room temperature", London.

[16] British Standards Institution, 2010, "BS EN ISO 148-1. Metallic materials – Charpy pendulum impact test – Part 1: Test method", London.

[17] Lakshminarayanan, A. K., and Balasubramanian, V., 2012, "Assessment of fatigue life and crack growth resistance of friction stir welded AISI 409M ferritic stainless steel joints", Mater. Sci. Eng. A, 539, pp. 143-153.

[18] Hobbacher, A., 2008, "Recommendations for Fatigue Design of Welded Joints and Components", International Institute of Welding, doc. IIW-1823-07, Paris.

[19] Gray, T., Camilleri, D., and McPherson, N., 2014, Control of Welding Distortion in Thin-Plate Fabrication, Woodhead Publishing, Cambridge, UK.

[20] He, X., Gu, F., and Ball, A., 2014, "A review of numerical analysis of friction stir welding", Prog. Mater. Sci., 65, pp. 1-66.

[21] Schmidt, H., Hattel, J., and Wert, J., 2004, "An analytical model for the heat generation in friction stir welding", Model. Simul. Mater. Sci. Eng., 12, pp. 143-157.

[22] Micallef, D., Camilleri, D., Toumpis, A., Galloway, A., and Arbaoui, L., 2015, "Local heat generation and material flow in friction stir welding of mild steel assemblies', Proc. Inst. Mech. Eng. Part L J. Mater. Des. Appl., pp. 1–17.

[23] Camilleri, D., Comlekci, T., and Gray, T. G. F., 2005, "Computational prediction of out-of-plane welding distortion and experimental investigation", J. Strain Anal. Eng. Des., 40, pp. 161-176.

[24] Camilleri, D., Mollicone, P., and Gray, T. G. F., 2007, "Computational methods and experimental validation of welding distortion models", Proc. Inst. Mech. Eng. Part L J. Mater. Des. Appl., 221, pp. 235-249.